Metal- and Ligation-Dependent Fragmentation of $[M(1,10\text{-Phenanthroline})_{1,2,3}]^{2+}$ Cations with M = Mn, Fe, Co, Ni, Cu, and Zn: Comparison between the Gas Phase and Solution

Janna Anichina, Xiang Zhao, and Diethard K. Bohme*

Department of Chemistry, Centre for Research in Mass Spectrometry and Centre for Research in Earth and Space Science, York University, Toronto, Ontario, Canada, M3J 1P3

Received: April 21, 2006; In Final Form: July 28, 2006

The core ions $[ML_n]^{2+}$ with $n = 1-3$, where L = 1,10-phenanthroline and M is a first-row transition metal, have been successfully transferred from aqueous solution into the gas phase by electrospraying and then probed for their stabilities by collision-induced dissociation in a triple quadrupole mass spectrometer. The triply ligated metal dications $[ML_3]^{2+}$ were observed to dissociate by the extrusion of a neutral ligand, while ligand loss from both $[ML_2]^{2+}$ and $[ML]^{2+}$ was accompanied by electron transfer. Comparisons are provided between gas-phase stabilities and stabilities for ligand loss measured in aqueous solution at 298 K. The measured onset for ligand loss from $[ML_3]^{2+}$ is quite insensitive to the metal, while a distinct stability order has been reported for aqueous solution. Low level density functional theory (DFT) calculations predict an intrinsic stability order for loss of ligand from $[ML_2]^{2+}$, but it differs from that in aqueous solution. Substantial agreement was obtained for the stability order for the loss of ligand from $[ML]^{2+}$ deduced from onset energies measured for charge separation, computed with DFT, and reported for aqueous solution where hydration seems less decisive in influencing this stability order. A qualitative potential-energy diagram is presented that allows the energy for charge separation to be related to the energy for neutral ligand loss from $[ML]^{2+}$ and shows that $IE(M^+)$ is decisive in determining the intrinsic stability order for loss of ligand from $[ML]^{2+}$.

1. Introduction

Important insights into the similarities and differences between ions in solution and in the gas phase can be obtained from experimental studies of the gas-phase stabilities of ions born in solution. Such studies have become feasible with the advent of electrospray ionization (ESI) mass spectrometry (MS).[1,2] A special opportunity arises when stabilities of (solvated) ions are well-known in solution and when their core ions remain intact in the electrospray process and so can be exposed to collision-induced dissociation in the gas phase. 1,10-Phenanthroline is a ligand that coordinates with first-row transition metal ions M^{2+} in aqueous solution with stability constants that are well-known.[3] Since the core ligated metal ion complexes survive the electrospray and can be collisionally dissociated, they are well suited for a comparative study of gas-phase and solution stabilities, and this is the focus of the work reported here.

Complexes of 1,10-phenanthroline and M^{2+} transition metal cations are well-known to play an important role in numerous biological processes, such as dioxygen transport,[4] in the biosynthesis of a variety of substances,[5] and in the killing of parasites in vivo.[6] When incorporated in polyamine macrocycles, 1,10-phenanthroline provides a basis for the investigation of molecular recognition of different substrates, including inorganic cations.[7,8] Furthermore, transition metal complexes with this molecule can exhibit high specificity and stereoselectivity in the binding to DNA, a property that is very desirable in the design of new efficient drugs and the creation of structural models of the existing drugs.[9,10]

Electrospray studies of the formation of $[ML_n]^{2+}$ dications with L = 1,10-phenanthroline have not been extensive. We are aware of a recent report of the observation of $[MnL_n]^{2+}$ with $n = 2$ and 3, $[MnL_nCl]^+$ with $n = 0-2$, and $[Mn_2L_nCl_3]^+$ with $n = 2$.[11] Collision-induced-dissociation (CID) spectra were recorded for these ions. Both charge separation by intracomplex electron transfer and losses of neutral ligands were observed, and the relative energies for these two processes were also computed using density functional theory (DFT) methods. An in-depth ESI/MS study of ion pairs of the type $[ML_nX]^+$ with L = 1,10-phenanthroline has been reported previously[12] for M = Mn(II), Fe(II), Co(II), Ni(II), Cu(II), and Zn(II) and X = Cl^-, NO_3^-, acetylacetonate, ClO_4^-, acetate, or SCN^-.

Here we employ ESI/CID mass spectrometry to investigate the gas-phase dissociation of doubly charged metal complexes of 1,10-phenanthroline, $[ML_n]^{2+}$, with up to three attached ligands ($n = 1-3$) and six different transition metal ions (M = Mn, Fe, Co, Ni, Cu, and Zn). We focus on the experimental determination of relative gas-phase stabilities by collision-induced dissociation and compare these to known stabilities in solution as well as computed gas-phase stabilities.

2. Experimental Section

Electrospray data were acquired in the positive ion mode using an API 2000 (MDS-SCIEX, Concord, ON, Canada) triple quadrupole ($Q_1q_2Q_3$) mass spectrometer equipped with a "Turbo Ion Spray" ion source. Experiments were performed at an ion spray voltage of 5500 V, a ring-electrode potential of 300 V (used for ion beam confinement), and a range of potential differences between the orifice and the skimmer. N_2 was used as a curtain gas at a setting of 10 psi, and air was used as a nebulizer at a flow rate of 8 L min^{-1}. Samples were directly infused into the electrospray source at a flow rate of 3 μL min^{-1}.

MS/MS was carried out in the product ion and multiple reaction monitoring (MRM) modes with N_2 as collision gas at

* Corresponding author. Phone: (416) 736-2100, ext 66188. Fax: (416) 736-5936. E-mail: dkbohme@yorku.ca.

10.1021/jp0624707 CCC: $33.50
Published on Web 08/29/2006

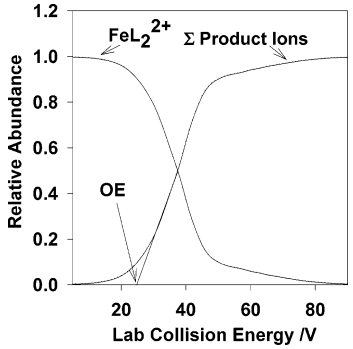

Figure 1. Determination of onset energy, OE, from the "refined curve" for the dissociation of doubly ligated metal dications, FeL_2^{2+}.

a pressure estimated to be about 3 mTorr (viz. multicollision conditions). The collision offset voltage (the potential difference between the quadrupole entrance lens (q_0) and the collision cell quadrupole (q_2)), which nominally gives the laboratory frame collision energy, was adjusted between 5 and 130 V at 1 V intervals. Space charge and contact potentials, field penetration, and field distortion all can influence the actual collision energy, but were not taken into account. The zero of energy was not measured. Product ion spectra were then obtained by scanning Q_3 over the range $m/z = 10-650$. The interquadrupole lens potentials and the float potential of the resolving quadrupole Q_3 were linked to the q_2 potential to maintain proper transmission through Q_3.

The onset energy of a particular primary dissociation was determined by extrapolating the steepest slope of a plot of the sum of the relative intensities of the primary dissociation products and their further fragments (the "refined curve") versus the applied collision energy to the *x*-axis, as shown in Figure 1. The precision of the onset energies is taken to be one standard deviation from the mean onset energy value obtained in several (four or more) repeated experiments. In each experiment Gaussian smoothing was applied twice to the ion signals measured at each collision voltage, each accumulated for a dwell time of 200 ms, to remove local variations caused by noise. We have chosen this approach over reporting separately the onsets for individual primary product ions. The inclusion of the further dissociation product ions improves the determination of the onset energy, especially for those primary ions that quickly dissociate further. For primary dissociations leading to charge separation, both primary product ions and their respective secondary and higher order fragment ions (if any) are all added together.

In the preparation of sample solutions, 1,10-phenanthroline was dissolved in a 1:1 water/methanol mixture at a concentration of 1 μM and the appropriate metal salt was added to 10-fold molar excess.

Ligated Cu(II), Zn(II), Co(II), Ni(II), and Mn(II) were generated from their nitrate hydrates (Aldrich, p.a $\geq$99.99%) without further purification. $FeSO_4 \cdot 7H_2O$ (Aldrich, p.a $\geq$98.%) was used as the source of Fe(II) ions. 1,10-Phenanthroline was purchased from Aldrich (p.a $\geq$98.%). HPLC degree methanol and Millipore (18.2 mΩ) water were used to prepare the solvent mixtures.

3. Computational Section

Low level density functional theory (DFT) calculations were carried out utilizing the Gaussian 98 program package,[13] and the B3LYP hybrid density function[14] was employed throughout. All of the metal atoms were described by a Lanl2dz basis set.[15−17] The 6-31G basis set[18] was used for C and H atoms. 6-31+G(d) was employed for N atom.[19−21] Various spin multiplicities were calculated for many of the species. All stationary points were characterized by harmonic vibrational frequency calculations, and these established that all the reported structures are at minima. Energies are corrected for zero point vibrational energy contributions.

4. Results and Discussion

4.1. Ions Emerging from the ESI Source. The nature of ions emerging from the ESI source was found to be quite sensitive to the declustering potential (DP), the potential applied to the orifice plate, in the range 0−200 V. This potential has the greatest effect on the amount of fragmentation in the orifice−skimmer region of the source area. The types of metal complexes that were observed in this range of DP are summarized in Table 1.

$[ML_3]^{2+}$ prevails at ca. 0 V, $[ML_2]^{2+}$ maximizes at ca. 30 V, and $[ML]^{2+}$ always is a relatively minor ion. An increase in DP above ca. 50 V leads to charge separation, neutral ligand loss from the triply ligated complexes, and ligand fragmentation.

In addition to $[ML_n]^{2+}$ dications, ion-pair complexes such as $[M^{2+}LNO_3^-]^+$ and $[M^{2+}L_2NO_3^-]^+$ were seen for M = Mn, Co, Ni, Cu, and Zn for which NO_3^- was the counterion in solution as first reported by Vachet and Callahan.[12] No ion pairs were observed with M = Fe for which the counterion in solution is SO_4^{2-}. We suppose that ion pairs are generated in the ESI process because of the tendency of metal ions to bond to as many ligands as necessary to saturate their coordination spheres. Formation of ion pairs may be increasingly favored in the electrospray process during solvent evaporation as the equilibrium in reaction 1 shifts toward formation of solvent molecules (to the right)

$$[ML_nS_m]^{2+} + [XS_l]^- \leftrightarrow [ML_nS_{m-1}X]^+ + S_{l+1} \qquad (1)$$

where M is the metal, L is 1,10-phenanthroline, $n = 1-3$, S is methanol and/or water, and X is NO_3^-.

$[ML(CH_3OH)]^{2+}$ is the only solvent cluster that was observed in the DP range from 0 to 60 V and was observed for all metals except Fe (see Table 1).

4.2. CID Profiles. CID profiles were measured for the $[ML_n]^{2+}$ ions with $n = 1-3$. The triply ligated metal dications were observed to dissociate by the extrusion of a neutral ligand according to reaction 2.

$$[ML_3]^{2+} \rightarrow [ML_2]^{2+} + L \qquad (2)$$

A further increase in the laboratory collision energy leads to the dissociation of $[ML_2]^{2+}$ and its primary products. This is illustrated in Figure 2 for the dissociation of [Co(1,10-phenanthroline)$_3$]$^{2+}$. All six metal complexes behaved in the same manner. The onset voltage of the primary dissociation (2) was observed to be relatively low (8−10 V) and quite independent of the metal (see Table 2).

In contrast to the dissociation of triply ligated metal dications, the dissociation of doubly and singly ligated metal dications was observed to proceed by charge separation according to reactions 3 and 4:

$$[ML_2]^{2+} \rightarrow [ML]^+ + L^+ \qquad (3)$$

$$[ML]^{2+} \rightarrow M^+ + L^+ \qquad (4)$$

This is illustrated for the dissociations of [Mn(1,10-phenanthroline)$_2$]$^{2+}$ and [Zn(1,10-phenanthroline)]$^{2+}$ in Figures 3 and

TABLE 1: Types of Metal Ion Complexes That Were Observed To Emerge from the ESI Source of an API 2000 Instrument at DP = 0−200 V[a]

ion[b]	Cu(II)	Zn(II)	Ni(II)	Co(II)	Mn(II)	Fe(II)
$[ML_2NO_3]^+$	•	•	•	•	•	
$[ML(CH_3OH)]^{2+}$	•	•	•	•	•	
$[MLNO_3]^+$	•	•	•	•	•	
$[MLNO]^+$	•		•	•	•	
$[MLO_2]^+$	•		•	•	•	
$[MLO]^+$	•	•	•	•	•	
$[ML]^+$	•	•	•	•	•	•
$[ML]^{2+}$	•	•	•	•	•	•
$[ML_2]^{2+}$	•	•	•	•	•	•
$[ML_3]^{2+}$	•	•	•	•	•	•

[a] The samples were electrosprayed at 10:1 metal ion:ligand (the concentration of the ligand being 1 μM) from solutions of 1:1 water:methanol. Ligated Cu(II), Zn(II), Co(II), Ni(II), and Mn(II) were generated from their nitrate hydrates while Fe(II) was generated from $FeSO_4 \cdot 7H_2O$. [b] L = 1,10-phenanthroline.

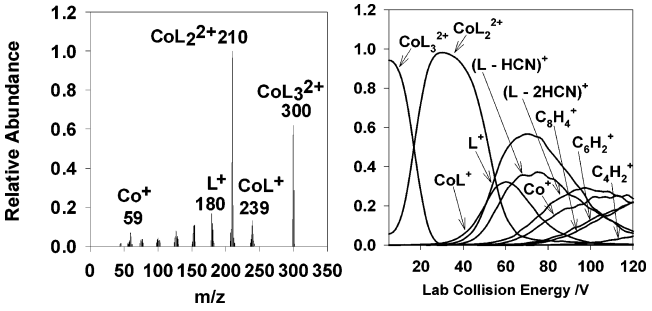

Figure 2. CID spectrum of $m/z = 300$ ($[CoL_3]^{2+}$) at 25 V and CID profiles monitored for the dissociation of $[CoL_3]^{2+}$ up to 120 V. L = 1,10-phenanthroline.

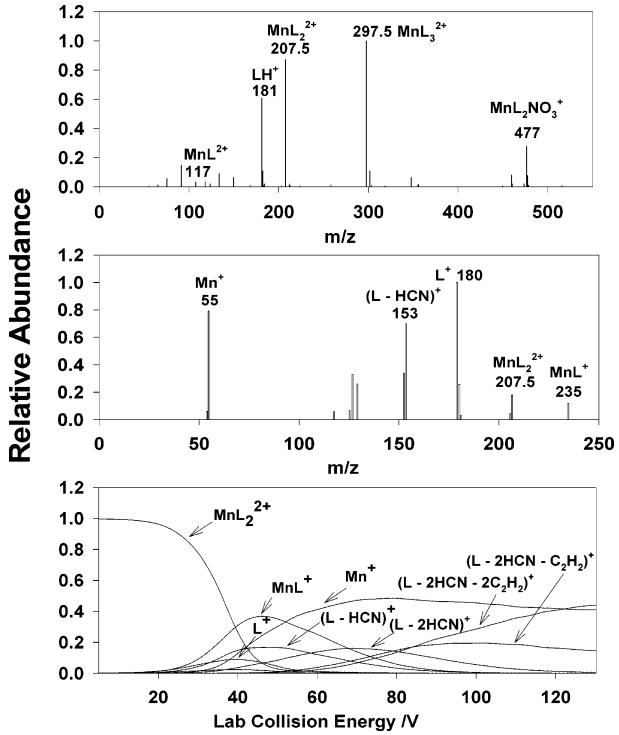

Figure 3. ESI spectrum of Mn(II)−1,10-phenanthroline (L) (top), CID spectrum of $m/z = 208$ ($[MnL_2]^{2+}$) at 50 V (middle), and CID profiles monitored for the dissociation of $[MnL_2]^{2+}$ (bottom).

4, respectively. The onsets for the dissociation reactions (3) and (4) were found to be metal dependent and those for (3) were always higher: 15−26 V compared to 5−15 V for (4) (see Table 2).

Notwithstanding the presence of a Coulomb barrier in the process of charge separation, the change from ligand loss (in the case of the dissociation of $[ML_3]^{2+}$) to charge separation (in the case of the dissociations of $[ML_2]^{2+}$ and $[ML]^{2+}$) can be understood in terms of the thermodynamics of these processes. Charge separation is more exothermic than ligand loss for the dissociation of ML^{2+} since the second ionization energies of the metals, viz. $IE(M^+)$, which are in the range 15.64 (for Mn) to 20.31 eV (for Cu), are much larger than the ionization energy of 1,10-phenanthroline. IE(L) = 8.51 eV. Charge separation still appears to be more exothermic than ligand loss in the dissociation of $[ML_2]^{2+}$, but since ligation makes $IE(ML^+) < IE(M^+)$, the attachment of three ligands to M^{2+} may render ligand loss more exothermic than charge separation in the dissociation of $[ML_3]^{2+}$.

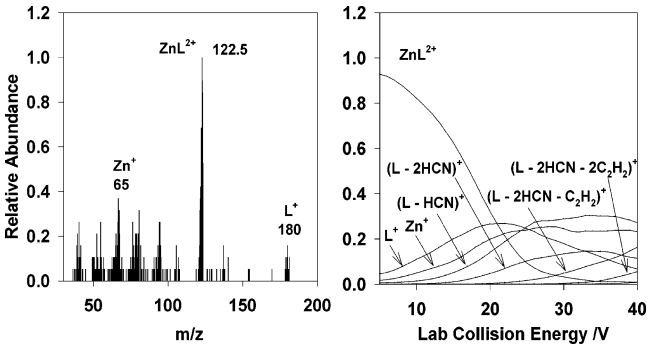

Figure 4. CID spectrum of $m/z = 122.5$ ($[ZnL]^{2+}$) at 20 V and CID profiles monitored for the dissociation up to 40 V. L = 1,10-phenanthroline. Ion collection appears to discriminate against the Zn^+ ion by a factor of about 2.4, presumably due to its relative velocity.

4.3. Dissociation of 1,10-Phenanthroline Cations. The dissociation of 1,10-phenanthroline cations yields ions with m/z = 153, 126, 100, 74, and 50, presumably according to reactions 5−9.

$$C_{12}H_8N_2^+ (180) \rightarrow C_{11}H_7N^+ (153) + HCN \quad (5)$$

$$C_{11}H_7N^+ (153) \rightarrow C_{10}H_6^+ (126) + HCN \quad (6)$$

$$C_{10}H_6^+ (126) \rightarrow C_8H_4^+ (100) + C_2H_2 \quad (7)$$

$$C_8H_4^+ (100) \rightarrow C_6H_2^+ (74) + C_2H_2 \quad (8)$$

$$C_6H_2^+ (74) \rightarrow C_4H_2^+ (50) + C_2 \quad (9)$$

The measured profiles do not preclude the formation of $C_4H_2^+$ directly from $C_8H_4^+$. The sum of the intensities of the 1,10-phenanthroline cation and its fragments is roughly equal to that of $[ML]^+$ and M^+, a result that is consistent with the stoichiometry of reaction 3.

TABLE 2: Measured Onset Energies for Dissociation Reactions 2−4 (See Text) and Second Ionization Energies of the Metals, IE(M^+)

	$[ML_3]^{2+} \rightarrow [ML_2]^{2+} + L$		$[ML_2]^{2+} \rightarrow [ML]^+ + L^+$		$[ML]^{2+} \rightarrow M^+ + L^+$		
	OE_{lab}[b]	OE_{CM}[c]	OE_{lab}[b]	OE_{CM}[c]	OE_{lab}[b]	OE_{CM}[c]	IE(M^+)[a]
Cu	8.8 ± 0.9	0.78	15.0 ± 0.9	1.86	5.5 ± 0.3	1.2	20.31
Ni	9.6 ± 0.9	0.86	20.3 ± 0.7	2.54	11.3 ± 0.7	2.38	18.17
Zn	9.3 ± 0.4	0.82	23.3 ± 0.4	2.88	14.1 ± 0.7	2.90	17.96
Co	9.7 ± 0.6	0.86	24.3 ± 0.5	3.04	13.1 ± 0.7	2.74	17.06
Fe	9.7 ± 0.4	0.87	25.3 ± 0.8	3.20	13.5 ± 0.5	2.86	16.18
Mn	9.3 ± 0.3	0.84	26.4 ± 0.5	3.34	14.5 ± 0.5	3.09	15.64

[a] Ionization energy of the metal cation in electronvolts.[22] IE(1,10-phenanthroline) = 8.51 eV.[22] [b] Measured onset energy in volts. [c] Apparent center-of-mass energy $OE_{CM} = (OE_{lab})zm(m + M)^{-1}$, where m represents the mass of the collision gas molecules (N_2), M is the mass of the molecular ion investigated, and z is the number of charges on the selected ion.

TABLE 3: Common Logarithms for the Binding Constants of Stepwise Coordination of the First-Row Transition Metal Cations (M^{2+}) Ligated with 1,10-Phenanthroline in Aqueous Solutions at 298 K and Ionic Strength $\mu = 0.1$[a]

M^{2+}	log K_1	log K_2	log K_3
Mn^{2+}	4.5	4.15	4.05
Fe^{2+}	5.86	5.25	10.03
Co^{2+}	7.02	6.7	6.28
Ni^{2+}	8.0	8.0	7.9
Cu^2	8.82	6.67	5.02
Zn^{2+}	6.3	5.65	5.1

[a] Data are taken from ref 3.

4.4. Comparison with Solution. Table 3 provides common logarithms of the binding constants for the stepwise coordination of first-row transition metal cations (M^{2+}) with 1,10-phenanthroline in aqueous solutions at 298 K and ionic strength $\mu = 0.1$.[3] These data provide a measure of the stability of the three states of coordination in solution.

The dissociation reaction (2) observed in the gas phase in our experiments mimics that in solution in that it involves the loss of one ligand. Also, the measured OE for the loss of one ligand in the gas phase represents the *intrinsic* stability of $[ML_3]^{2+}$. Our measurements summarized in Table 2 indicate that the onset energies for the loss of L from $[ML_3]^{2+}$, and so the intrinsic stabilities of $[ML_3]^{2+}$, are quite independent of the nature of M in the gas phase as one might expect if the third ligand is electrostatically bound. In contrast to the gas phase, the values for log K_3 in Table 3 indicate that this is not the case in aqueous solution, where the order of stability is Mn(II) < Cu(II) ≈ Zn(II) < Co(II) < Ni(II) < Fe(II). Apparently the relative hydration energies of $[ML_2]^{2+}$ and $[ML_3]^{2+}$ are sufficiently different from each other to introduce the observed metal dependence of K_3 in solution.

The Irving−Williams series, Mn(II) < Fe(II) < Co(II) < Ni(II) < Cu(II) > Zn(II), which is frequently used to describe the relative stabilities of first-row transition metal complexes in solution,[23] coincides only with the order in log K_1 given in Table 3, viz. the order of stability of the singly ligated species in solution. Our measurements indicate that the singly ligated $[ML]^{2+}$ dissociates in the gas phase by charge separation rather than the loss of the neutral ligand. Nevertheless, as we shall now show, a thermodynamic analysis is possible that allows a direct comparison of the stability order for neutral ligand loss from ML^{2+} in the gas phase with the Irving−Williams series in solution.

4.5. Thermodynamics of the Dissociation of $[ML]^{2+}$. The thermodynamic parameters that determine the intrinsic stability of $[ML]^{2+}$ are illustrated qualitatively in the potential-energy diagram shown in Figure 5.

Figure 5 shows that the thermodynamic onset energy, OE_{TD}, for the dissociation of $[ML]^{2+}$ by charge separation, reaction 4, is comprised of the energy required to separate the charge,

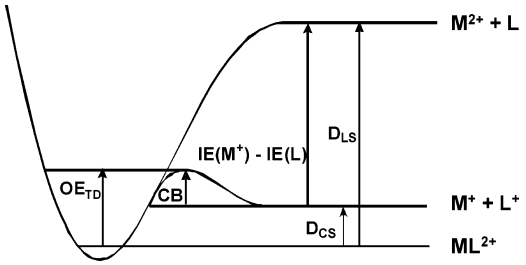

Figure 5. Qualitative potential-energy diagram for ligand and charge separation for singly ligated doubly charged metal ions. OE_{TD} is the thermodynamic onset energy, CB denotes the Coulomb barrier, IE(M^+) is the second ionization energy of the metal, IE(L) is the ligand ionization energy, D_{LS} is the energy for ligand separation, and D_{CS} is the energy for charge separation.

TABLE 4: Comparison of Calculated and Experimental Ionization Energies, IE (in eV), at the B3LYP/LanL2dz Level of Theory[a]

	first IE		second IE	
M	calcd	exptl	calcd	exptl
Mn	7.88	7.43402	15.30	15.63999
Fe	7.17	7.9024	16.74	16.1878
Co	8.84	7.8810	16.44	17.083
Ni	7.76	7.6398	20.41	18.16884
Cu	7.83	7.72638	20.80	20.29240
Zn	9.17	9.3942	17.21	17.96440

[a] Experimental values are from ref 24.

D_{CS}, and the energy required to surmount the Coulomb barrier, CB, associated with this process according to eq 10.

$$OE_{TD} = D_{CS} + CB \tag{10}$$

If CB is assumed to be the same for all six singly ligated complexes due to the electrostatic nature of the Coulomb barrier, then, to a good approximation, the *order* in OE_{TD} will give the *order* in the bond dissociation energy, D_{CS}.

If we assume that the measured onset energy OE for charge separation expressed as OE_{CM} is equal to OE_{TD}, an order in D_{CS} of Mn ≥ Zn ∼ Fe ≥ Co > Ni > Cu is obtained (see Table 2). However, the approximation that $OE_{CM} = OE_{TD}$, even under single-collision conditions, ignores any internal energies of the electrosprayed ions as well as the kinetic energy distributions of the colliding species and differences in rates of dissociation of the metal complexes. Our results are not obtained under single-collision conditions, and we cannot exclude the presence of some internal excitation in the electrosprayed ions.

According to Figure 5, the energy required to remove a ligand from $[ML]^{2+}$ without charge separation, D_{LS}, is related to D_{CS} by eq 11.

$$D_{LS} = D_{CS} + IE(M^+) - IE(L) \tag{11}$$

TABLE 5: Absolute Energies (in hartrees at 0 K) and Electronic States for the Lowest Energy States of M^+, M^{2+}, $[ML]^+$, $[ML]^{2+}$, and $[ML_2]^{2+}$ Provided by Theory[a,b]

M	M^+		M^{2+}		ML^+		ML^{2+}		ML_2^{2+}	
Mn	^{7}S	−103.599	^{6}S	−103.037	^{7}A$_1$	−675.067	^{6}A$_1$	−674.711	^{6}A$_2$	−1246.231
Fe	^{4}F	−123.095	^{5}D	−122.480	^{4}B$_2$	−694.557	^{5}A$_1$	−694.187	^{5}A$_2$	−1265.720
	^{6}D	−123.069			^{6}B$_1$	−694.544				
Co	^{5}F	−144.692	^{4}F	−144.088	^{3}B$_2$	−716.194	^{4}B$_2$	−715.785	^{4}B$_1$	−1287.360
	^{3}F	−144.685			^{5}B$_1$	−716.180				
Ni	^{2}D	−168.962	^{3}F	−168.212	^{2}A$_2$	−740.467	^{3}B$_2$	−740.014	^{3}A$_1$	−1311.566
Cu	^{1}S	−195.829	^{2}S	−195.065	^{1}A$_1$	−767.315	^{2}B$_1$	−766.880	^{2}B$_1$	−1338.393
Zn	^{2}S	−65.259	^{1}S	−64.626	^{2}A$_1$	−636.729	^{1}A$_1$	−636.347	^{1}A$_1$	−1207.875

[a] 1,10-Phenanthroline has a ground state of ^{1}A$_1$ with E + ZPE = −571.325; 1,10-phenanthroline$^+$ has a ground state of ^{2}B$_2$ with E + ZPE = −571.027. [b] L = 1,10-phenanthroline.

TABLE 6: Computed Values for IE(ML^+) (in eV) and Dissociation Energies at 0 K (in kcal mol^{-1}) for $[ML]^+$, $[ML]^{2+}$, and $[ML_2]^{2+}$, with L = 1,10-Phenanthroline[a]

dissociation channel		Mn	Fe	Co	Ni	Cu	Zn
1	$ML^+ \rightarrow M^+ + L$	89.7	85.2[b]	110.5[c]	112.4	100.8	91.1
			101.7[d]	115.3[e]			
	IE(ML^+)	9.7	10.1	11.1	12.3	11.8	10.4
2	$ML^{2+} \rightarrow M^{2+} + L$	218.9	239.4	232.6	298.6	307.6	247.9
3	$ML^{2+} \rightarrow M^+ + L^+$	53.2	40.7[f]	40.8[g]	15.1	15.2	38.1
			57.2[h]	45.6[i]			
	OE_{CM}[a]	73.8	69.2	63.2	54.4	26.2	66.8
4	$ML_2^{2+} \rightarrow ML^+ + L^+$	86.0	85.5[j]	87.1[k]	45.5	31.9	74.4
			93.3[l]	94.1[m]			
	OE_{CM}[a]	76.6	73.8	69.2	58.6	43.0	65.6
5	$ML_2^{2+} \rightarrow ML^{2+} + L$	122.4	130.0	156.8	142.7	117.5	127.4

[a] Experimental values for OE_{CM} (in kcal mol^{-1}) from Table 2 are included for comparison. [b] $FeL^+(^4B_2) \rightarrow Fe^+(^4F) + L$. [c] $CoL^+(^3B_2) \rightarrow Co^+(^5F) + L$. [d] $FeL^+(^4B_2) \rightarrow Fe^+(^6D) + L$. [e] $CoL^+(^3B_2) \rightarrow Co^+(^3F) + L$. [f] $FeL^{2+}(^5A_1) \rightarrow Fe^+(^4F) + L^+$. [g] $CoL^{2+}(^4B_2) \rightarrow Co^+(^5F) + L^+$. [h] $FeL^{2+}(^5A_1) \rightarrow Fe^+(^6D) + L^+$. [i] $CoL^{2+}(^4B_2) \rightarrow Co^+(^3F) + L^+$. [j] $FeL_2^{2+}(^5A_2) \rightarrow FeL^+(^4B_2) + L^+$. [k] $CoL_2^{2+}(^4B_1) \rightarrow CoL^+(^3B_2) + L^+$. [l] $FeL_2^{2+}(^5A_2) \rightarrow FeL^+(^6B_1) + L^+$. [m] $CoL_2^{2+}(^4B_1) \rightarrow CoL^+(^5B_1) + L^+$.

Therefore, for a family of dissociations involving the same L but different M, eq 12 applies.

$$\Delta D_{LS} = \Delta(OE_{TD} + IE(M^+)) \qquad (12)$$

Equation 12 indicates that the order in ligation energy of doubly charged $[ML]^{2+}$ ions can be deduced simply from measurements of OE_{TD} for charge separation when the ionization energies IE(M^+) are known! Equation 12 predicts the order Cu(II) > Zn(II) > Ni(II) > Co(II) > Fe(II) > Mn(II). Except for the relative position of Zn(II), the intrinsic order obtained in this way is the same as the order in aqueous solution, viz. Cu(II) > Ni(II) > Co(II) > Zn(II) > Fe(II) > Mn(II) (see Table 3). This implies in turn that differences in the hydration energy of $[ML]^{2+}$ and M^{2+} in aqueous solution are not very effective in altering the intrinsic order of stability for ligand loss.

4.6. Computations of Intrinsic Stabilities. To gain further insight into the intrinsic energetics of ligand loss from the metal complexes with and without concomitant electron transfer, all of the relevant species were investigated theoretically using density functional theory. A sense of the accuracy of the calculations can be gleamed from the comparison of calculated and experimental ionization energies at the B3LYP/LanL2dz level of theory given in Table 4. The deviations can be quite large and are largest for IE(Fe,Co) and IE(Ni^+,Zn^+).

All of the possible spin multiplicities for all of the cations M^+, M^{2+}, ML^+, ML^{2+}, and ML_2^{2+} were investigated. Table 5 lists the energies associated with the states found to be lowest in energy. These states correspond to ground states except Co^+(^{5}F), which is lower in energy by 4.8 kcal mol^{-1} than the Co^+(^{3}F) ground state, and Fe^+(^{4}F), which is lower in energy by 16.5 kcal mol^{-1} than the Fe^+(^{6}D) ground state. This can be attributed to the poor quality of the Gaussian 98 calculation with the LanL2dz basis set.

All of the singly charged and doubly charged monoligated complexes were found to be planar. All of the doubly ligated dications $[ML_2]^{2+}$, with the exception of $[CuL_2]^{2+}$, were found to have D_{2d} symmetry and tetrahedral-like coordination; i.e., the planes of the two 1,10-phenanthroline ligands are perpendicular to each other. CuL^{2+} was found to have D_2 symmetry in which the dihedral of the two ligand planes is 41°.

Table 5 lists the computed absolute energies at 0 K for the lowest energy states of M^+, M^{2+}, $[ML]^+$, $[ML]^{2+}$, and $[ML_2]^{2+}$. Table 6 provides the bond dissociation energies (BDE) at 0 K for M^+−L, M^{2+}−L, and ML^{2+}−L (channels 1, 2, and 5, respectively) and the charge separation energies for $[ML]^{2+}$ and $[ML_2]^{2+}$ (channels 3 and 4, respectively). Note that the binding energies that involve Fe^+ and Co^+ are referenced to Fe^+(^{4}F) and Co^+(^{5}F), respectively (see Table 6), which are computed to be the lowest energy states for these ions (but are excited states according to experiment). Our calculated bond dissociation energies for Mn^+−1,10-phenanthroline and Mn^{2+}−1,10-phenanthroline of 89.7 and 218.9 kcal mol^{-1} are close to the values of 81.6 and 219.1 kcal mol^{-1}, respectively, obtained at *m*PW1PW91/DZP level by Schröder and Schwarz.[25]

The calculations predict that the ligated dications $[ML]^{2+}$ are bound more than twice as strongly against loss of L than the monocations. This can be attributed to two effects: (i) the higher charge of the dication increases electrostatic bonding and (ii) the ground-state configuration of $M^{2+}(4s^03d^n, n = 5-10)$ allows for a better approach of the ligand than does $M^+(4s^13d^n, n = 5-10)$ in which the occupied 4s orbital is partially repulsive as is the case with $Mn^+(^7S,s^1d^5)$, $Fe^+(^6D,s^1d^6)$, and $Zn^+(^2S,s^1d^6)$.

The computed values for BDE of $[ML]^{2+}$ for the loss of neutral L (channel 2 in Table 6) range from 218.9 to 307.6 kcal mol^{-1}, whereas the charge separation to afford L^+ and high-spin M^+ (channel 3 in Table 6) is endothermic by only 15.1−53.2 kcal mol^{-1}. Similar results were obtained for the biligated

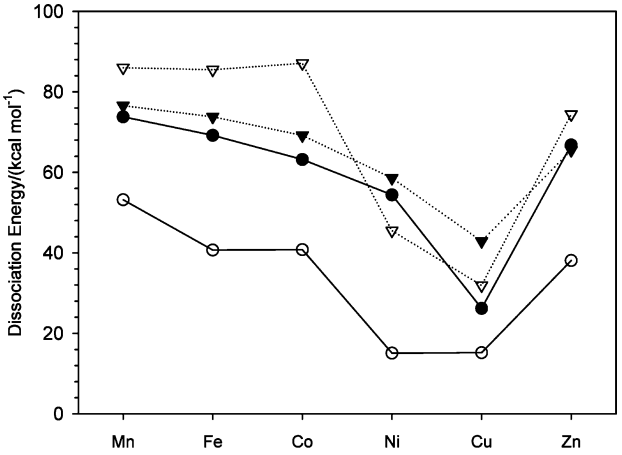

Figure 6. Comparison of computed values for D_{CS} with experimental values for OE_{CM}. Open triangles and open circles are computed values for D_{CS} of $[ML_2]^{2+}$ and $[ML]^{2+}$, respectively, with the latter being the lowest computed dissociation energies (see Table 6). Closed triangles and closed circles are experimental values for OE_{CM} of $[ML_2]^{2+}$ and $[ML]^{2+}$, respectively.

dications $[ML_2]^{2+}$. Hence, $[ML]^{2+}$ and $[ML_2]^{2+}$ are all thermochemically stable dications.[25,26] Thus the exclusive observation of charge separation in the CID of $[ML_2]^{2+}$ (Figures 2−4) indicates that CID favors the least endothermic dissociation even in the presence of a Coulombic barrier to charge separation in the systems investigated here.[11]

The comparison between the calculated values of D_{CS} and the measured OE_{CM} values is shown in Figure 6. It is seen that the trends in D_{CS} and the measured OE_{CM} are similar across the row of transition metals with a minimum for the bonding involving Cu. However, there are discrepancies in the absolute values and the possible causes for these are not straightforward to assess. The uncertainties in the calculations are not known, and the OE_{CM} values do not correspond to single-collision conditions and involve uncertainties of the type discussed earlier in this text. In ideal single-collision dissociation involving thermal ions, $OE_{CM} = CB + D_{CS}$ and D_{CS} should be less than OE_{CM} (although multiple-collision conditions and excess internal energy in the sprayed ions will act to reduce the apparent OE_{CM}). Figure 6 shows that $D_{CS} < OE_{CM}$ for the dissociation of $[ML]^{2+}$ with CB approximately equal to 25 ± 15 kcal mol^{-1}. In contrast, for the dissociation of doubly ligated $[ML_2]^{2+}$, Figure 6 shows CB to be much smaller, equal to approximately 0 ± 15 kcal mol^{-1}. This latter result is physically unreasonable since CB cannot be zero or negative and so points to shortcomings in the experiment and/or the calculations.

The calculated ligation energies listed in Table 6 for $[ML_2]^{2+}$ are in the order Co(II) > Ni(II) > Fe(II) > Zn(II) > Mn(II) > Cu(II). This order does not reproduce the stability order measured in aqueous solution, viz. Fe(II) > Ni(II) > Co(II) > Zn(II) > Cu(II) > Mn(II), and should not if solvation plays a decisive role in solution. For $[ML]^{2+}$ the computed order is Cu(II) > Ni(II) > Zn(II) > Fe(II) > Co(II) > Mn(II). This order (in which Fe(II) and Co(II) are closest to each other) compares favorably with the order in IE(M^+), viz. Cu(II) > Ni(II) > Zn(II) > Co(II) > Fe(II) > Mn(II), and the order based on the measurements of onset energies using eq 12, viz. Cu(II) > Zn(II) > Ni(II) > Co(II) > Fe(II) > Mn(II).

5. Conclusions

An opportunity has been grasped to compare solution and gas-phase stabilities of ions using electrospray mass spectrometry. Our data show that the core ions $[ML_n]^{2+}$ with $n = 1-3$, where L = 1,10-phenanthroline, and M are first-row transition metals, can be successfully transferred from aqueous solution into the gas phase by electrospraying and then probed for their stabilities by collision-induced dissociation.

The CID onsets measured for ligand loss from $[ML_3]^{2+}$ ions in the gas phase indicate no measurable differences in stability for the five transition metals investigated. This is in contrast to the observed stability order in aqueous solution which, as a consequence, can be attributed to differential solvation of reactant and product ions in solution.

Charge separation, as a result of ligand loss with concomitant electron transfer, is the predominant dissociation observed under CID conditions, while ligand loss occurs in solution. Nevertheless, thermodynamic considerations indicate that measured onset energies for charge separation relate to ligation energies for the singly ligated species ML^{2+} when the ionization energies IE(M^+) are known. In fact, the order in D_{LS} in the gas phase is determined mainly by IE(M^+), viz. Cu(II) > Ni(II) > Zn(II) > Co(II) > Fe(II) > Mn(II). Measured onset energies change this order only slightly to Cu(II) > Zn(II) > Ni(II) > Co(II) > Fe(II) > Mn(II), in which Ni(II) and Zn(II) have traded places. The intrinsic order obtained in this way compares well with that in aqueous solution, viz. Cu(II) > Ni(II) > Co(II) > Zn(II) > Fe(II) > Mn(II). This implies in turn that differences in the hydration energies of ML^{2+} and M^{2+} in aqueous solution are largely not effective in altering the intrinsic order of stability for ligand loss in ML^{2+} and so are small.

Low level DFT calculations that predict the order Cu(II) > Ni(II) > Zn(II) > Fe(II) > Co(II) > Mn(II) for the ligand loss in $[ML]^{2+}$ are able to reproduce reasonably well the order based on IE(M^+), viz. Cu(II) > Ni(II) > Zn(II) > Co(II) > Fe(II) > Mn(II), and the order based on the measurements of onset energies using eq 12, viz. Cu(II) > Zn(II) > Ni(II) > Co(II) > Fe(II) > Mn(II). The computed order in the intrinsic ligation energy of $ML^{2+}-L$, viz. Co(II) > Ni(II) > Fe(II) > Zn(II) > Mn(II) > Cu(II), does not reproduce the stability order measured in aqueous solution, viz. Fe(II) > Ni(II) > Co(II) > Zn(II) > Cu(II) > Mn(II), in which hydration appears to be decisive in determining these relative stabilities.

Acknowledgment. Continued financial support from the Natural Sciences and Engineering Research Council of Canada is greatly appreciated. Also, we acknowledge support from the National Research Council, the Natural Sciences and Engineering Research Council, and MDS SCIEX in the form of a Research Partnership grant. As holder of a Canada Research Chair in Physical Chemistry, D.K.B. thanks the Canada Research Chair Program for its contributions to this research. The authors also thank Michael J. Y. Jarvis, Voislav Blagojevic, and Tuba Gozet for their contributions.

References and Notes

(1) Yamaha, M.; Fenn, J. B. *J. Phys. Chem.* **1984**, *88*, 4451.

(2) Fenn, J. B. *J. Am. Soc. Mass Spectrom.* **1993**, *70*, 2348.

(3) *NIST Critical Stability Constants of Metal Complexes*, Version 8; National Institute of Standards and Technology: Washington, DC, 2004.

(4) Frausto da Silva, J. J. R.; Williams R. J. P. In *The Biological Chemistry of the Elements: the Inorganic Chemistry of Life*; Clarendon Press: Oxford, 1991.

(5) Cooper, C. E. In *Proc. Free Radical Damage and its Control*; Rice-Evans, C. A., Burdon, R. H., Eds.; Elsevier Science B.V.: Amsterdam, 1994; p 67.

(6) Slingaard, A.; Mahoney, J. R. J. *J. Biol. Chem.* **1991**, *266*, 4903.

(7) Bencini, A.; Bianchi, A.; Giorgi, C.; Fusi, V. *J. Org. Chem.* **2000**, *65*, 7686−7689

(8) Bazziculapi, C.; Bencini, A.; Fusi, V.; Giorgi, C.; Paolette, P.; Valtancoli, B. *Inorg. Chem.* **1998**, *37*, 941−948.
(9) Turro, N.; Barton, J.; Tomalia, D. *Acc. Chem. Res.* **1991**, *24*, 332−340.
(10) Barto, J.; Danishefsky, A.; Goldberg, J. *J. Am. Chem. Soc.* **1984**, *106*, 2172−2176.
(11) Tsierkezos, N. G.; Diefenbach, M.; Shröder, D.; Schwarz, H. *Inorg. Chem.* **2005**, *44*, 4969.
(12) Vachet, R. W.; Callahan, J. H. *J. Mass Spectrom.* **2000**, *35*, 311.
(13) Frisch, M. J.; Trucks, G. W.; Schlegel, H. B.; Scuseria, G. E.; Robb, M. A.; Cheeseman, J. R.; Zakrzewski, V. G.; Montgomery, J. A., Jr.; Stratmann, R. E.; Burant, J. C.; Dapprich, S.; Millam, J. M.; Daniels, A. D.; Kudin, K. N.; Strain, M. C.; Farkas, O.; Tomasi, J.; Barone, V.; Cossi, M.; Cammi, R.; Mennucci, B.; Pomelli, C.; Adamo, C.; Clifford, S.; Ochterski, J.; Petersson, G. A.; Ayala, P. Y.; Cui, Q.; Morokuma, K.; Malick, D. K.; Rabuck, A. D.; Raghavachari, K.; Foresman, J. B.; Cioslowski, J.; Ortiz, J. V.; Baboul, A. G.; Stefanov, B. B.; Liu, G.; Liashenko, A.; Piskorz, P.; Komaromi, I.; Gomperts, R.; Martin, R. L.; Fox, D. J.; Keith, T.; Al-Laham, M. A.; Peng, C. Y.; Nanayakkara, A.; Challacombe, M.; Gill, P. M. W.; Johnson, B.; Chen, W.; Wong, M. W.; Andres, J. L.; Gonzalez, C.; Head-Gordon, M.; Replogle, E. S.; Pople, A. J. A. *Gaussian 98*, revision A.11.4; Gaussian, Inc.: Pittsburgh, PA, 2002.
(14) Becke, A. D. *J. Chem. Phys.* **1993**, *98*, 5648.
(15) Wadt, W. R.; Hay, P. J. *J. Chem. Phys.* **1985**, *82*, 284.
(16) Hay, P. J.; Wadt, W. R. *J. Chem. Phys.* **1985**, *82*, 270.
(17) Hay, P. J.; Wadt, W. R. *J. Chem. Phys.* **1985**, *82*, 299.
(18) Hehre, W. J.; Ditchfie, R.; Pople, J. A. *J. Chem. Phys.* **1972**, *56*, 2257.
(19) Harihara, P.; Pople, J. A. *Theor. Chim. Acta* **1973**, *28*, 213.
(20) Krishnan, R.; Binkley, J. S.; Seeger, R.; Pople, J. A. *J. Chem. Phys.* **1980**, *72*, 650.
(21) Clark, T.; Chandrasekhar, J.; Spitznagel, G. W.; Schleyer, P. V. *J. Comput. Chem.* **1983**, *4*, 294.
(22) webbook.nist.gov.chemistry.
(23) Irving, H.; Williams, R. J. O. *J. Chem. Soc.* **1953**, 3192.
(24) Lide, D. R. *CRC Handbook of Chemistry and Physics*, 85th ed.; CRC Press: Boca Raton, FL, 2005.
(25) Schröder, D.; Schwarz, H. *J. Phys. Chem. A* **1999**, *103*, 7385.
(26) Stace, A. J. *J. Phys. Chem. A* **2002**, *106*, 7993.